Towards a Twisted String Actuated Haptic Device: Experimental Testing of a 2-D Virtual Environment and Teleoperation Interface

Linda Feenstra[1], Umberto Scarcia[2], Riccardo Zanella[2], Roberto Meattini[2], Davide Chiaravalli[2], Gianluca Palli[2] and Claudio Melchiorri[2]

***Abstract*— In the article, a first stage implementation of a haptic device towards a complete 3-D workspace twisted-string actuated haptic interface is discussed. In the present work, a 2-D setup is presented, with the aim of preliminarly testing the behaviour of this novel haptic system, especially with respect to the adopted cable-based actuation solution. In particular, the component descriptions, kinematics of the planar device and the controller for teleoperation purposes are illustrated. Results regarding the behaviour of the system in rendering a virtual environment and in a robot teleoperation scenario with haptic force feedback are reported. The experimental outcomes show that the designed and implemented system is suitable for teleoperation with haptic interfaces, providing positive perspectives for the realization of the fully functional 3-D haptic interface in the future work.**

I. Introduction

Nowadays, despite an ever increasing autonomy in robots, teleoperation still play a central role in the development and research of advanced robotics solutions. The reason of this can be found in the importance and necessity of involving the human operator's perception and decision making skills into the control loop for the regulation of remote robots. Important related applications can be found in the field of underwater, space missions, manipulation/exploration of dangerous materials/environments and surgery [1].

To this purpose, adequate human-machine interfaces are needed in order to provide to the teleoperation user proper physical information about the remote robot behaviour and operation. This especially holds for applications that include interaction with both virtual and real environments, in which the availability of interfaces able to provide sufficient force rendering plays a crucial role. This is the case of *haptic* devices aiming at providing to the user a feeling of *telepresence* – i.e. the perception of being physically present at the remote site – within the well-known *master-slave* paridigm in bilateral robotic teleoperation [2].

The evolution of this field have brought in the last decades to the development of several haptic devices for various teleoperation applications, including solution from academic laboratories and/or currently available on the market. Among the more widely used commercial haptic devices, we can mention the 6-DoF *Phantom OmniR* [3] (also commercialized as Geomagic Touch [4].); the haptic devices based on parallel structures by Falcon [5] and Force Dimension (*omega.x* and *delta.x*) [6] and kinematic chains with force feedback (*sigma.7*); the admittance-controlled haptic interface *MOOG* by HapticMaster [7]. Similarly, looking at the academic literature, also many researchers have proposed haptic devices using serial and parallel mechanisms: [8] and [9] presented a gimbal-based haptic parallel mechanism; in [10] four Phantom Omni are combined in order to provide a 6-Dof force rendering; a general purpose "joystick-like" haptic interface is illustrated in [11]; a specific haptic device for mobile manipulators is presented in [12], composed by two parallel mechanisms; in [13] a planar haptic device minimizes the impedance by means of a 5 bar linkage mechanism.

In general, it is worth to highlight that haptic devices with serial kinematic chains presents several well-known drawbacks. Indeed, this kind of devices are characterized by high inertia, reduced workspace and high mechanical complexity, resulting in limited manipulability for an effective usage and high costs of the device. Differently, an haptic device for teleoperation purposes should show very low inertia in order to allow a realistic reconstruction of the forces experienced by the slave robot [14]. One promising solution to overcome these problems is the usage of cable transmissions [15], [16] in the design of the haptic interface devices, since they provide remarkable force-weight ratios and low contribution to the device's end-point inertia. Several design strategies have been considered in recent studies for the development of cable driven haptic devices [17], [18], [19]. In the context of the present work, we are interested in the Twisted String Actuation (TSA) solution [20]: a very compact, lightweight and low cost cable-based linear transmission system. In literature, the TSA has been successfully used for the development of different robotic devices such as artificial hands [21], [22], grounded/wearable elbow [23], [24] and wearable dual arm [25] assistive devices and tensegrity robots for space applications [26]. In particular, recent previous works from our research group have presented a TSA module for highly-integrated mechatronic devices [27], and a preliminary, simulative study on the development of a TSA-based haptic interface carried out by Pepe et al. [28].

In this paper, a first-stage implementation of the TSA-based haptic interface theoretically designed and simulated in [28] is presented and preliminary evaluated experimentally.

[1]DME - Department of Mechanical Engineering, Eindhoven University of Technology, 5600 MB Eindhoven, Netherlands

[2]DEI - Department of Electrical, Electronic and Information Engineering, University of Bologna, Bologna, Italy

This work was supported by the European Commission's Horizon 2020 Framework Programme with the project REMODEL - Robotic technologies for the manipulation of complex deformable linear objects - under Grant 870133

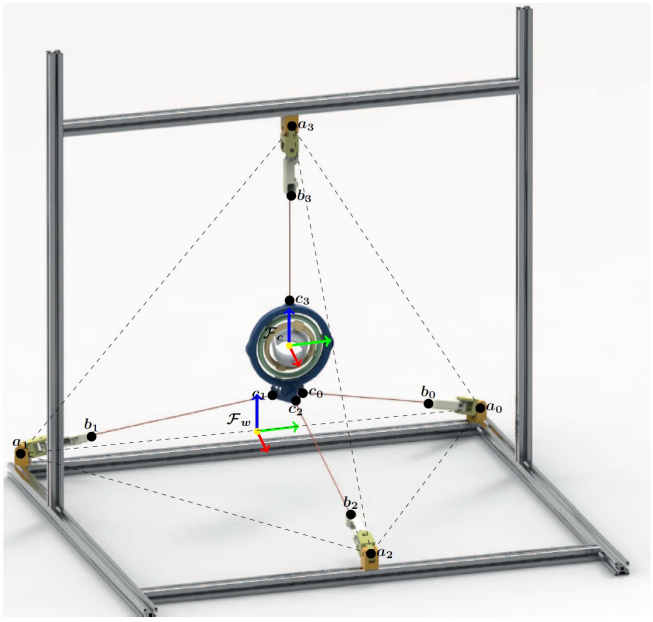

Fig. 1. CAD representation of the 3-D haptic interface presented in [28].

In particular, a planar version of this haptic interface was implemented using three TSA modules (instead of four TSA modules which are required for the full 3-D space device) and tested in order to evaluate the effectiveness and actual functioning of the system. The main contribution of this study is the actual implementation of a twisted string based haptic interface in a planar configuration, that includes the mechatronic realization and control design to achieve experimental force rending demonstrations. The article illustrates the system used in this work, and reports the results of an evaluation in two different experimental situation: the realization of a virtual environment in which a virtual wall is implemented by using force rendering, and a simple teleoperation scenario where the Baxter robot [29] is remotely controlled and the force exchanged with the environment is fed back to the user by the our 2-D haptic interface. The paper is organized as follows: in Sec. II the setup and the controller of the haptic device are illustrated; in Sec. III the experimental testing is presented and the related results reported; finally, Sec. IV outlines conclusive considerations.

II. Materials and Methods

The present work has to be intended as a first step towards the development of the complete three dimensional haptic interface visible in Fig. 1, composed by four TSA modules connected to a gimbal-based bracelet. In this paper, an important intermediate 2-D implementation of the system (observable in Fig. 3, refer also to Subsec. II-B) composed by three TSA modules and a handle carriage – the latter in place of the gimbal-bracelet – is reported and preliminary tested.

A. TSA Module

The TSA modules employed in this work are specifically designed for a cable-based force rendering haptic interface,

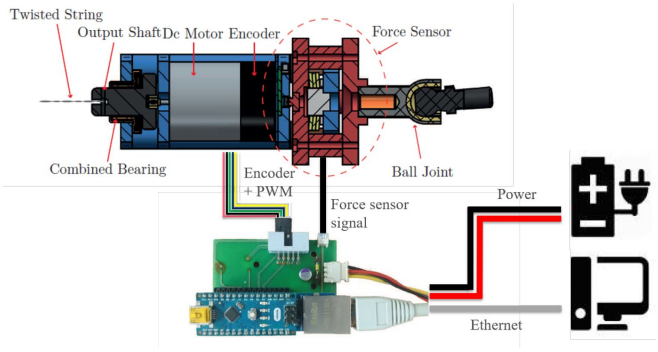

Fig. 2. The TSA module, embedded controller and connections.

and for detailed information it is possible to refer to our previous work [27]. Briefly, they are composed by an integrated force sensor, DC motor with encoder, embedded microcontroller and power electronics. The concept behind this twisted string actuator is simple: the rotary motion of the DC motor implies the twisting of a string connected to the output shaft: in this way the string changes its length. This behaviour can therefore be used to apply forces to a load at the opposite side of the string. A remarkable feature of these TSA modules is the integrated ultra-light low-power force sensing based on Belleville springs deformations [30], that are detected by optoelectronic components. Therefore, a reference force profile can be tracked by the TSA module, which, in turn, is equipped by a standard PID low level controller. Fig. 2 shows the TSA module with a qualitative schematic of its components and electrical connections.

B. 2-D Haptic Interface Setup

A haptic interface has been developed to remotely control a robotic arm in the two dimensional space and provide to the human operator the force feedback correspondent to the interaction between the robot and the environment. The proposed interface, as shown in Fig. 3, consists of three TSA modules named TSA_1, TSA_2 and TSA_3, that are placed in the corners of an equilateral triangle at attachment points a_0, a_1 and a_2, respectively (see Fig. 3). The TSA modules are also attached to a string at their output shafts at connection points b_0, b_1 and b_2. The strings, in turn, are connected to a carriage named Haptic Interface Carriage (HIC) (see Fig. 3) at the anchor points c_0, c_1 and c_2. The choice of the anchor points is motivated by ergonomic considerations. The small motion induced on the HIC by the rotation of the springs is easily compensated by the human operator without hindering the perception provided by the device. Therefore, thanks to the action of the TSA modules, the user of the haptic system can receive feedback forces and send position commands while holding and moving the HIC (further details in Subsec. II-C).

C. Haptic Interface Teleoperation Controller

In this subsection, the controller implemented for the 2-D haptic interface is illustrated. This controller must be able

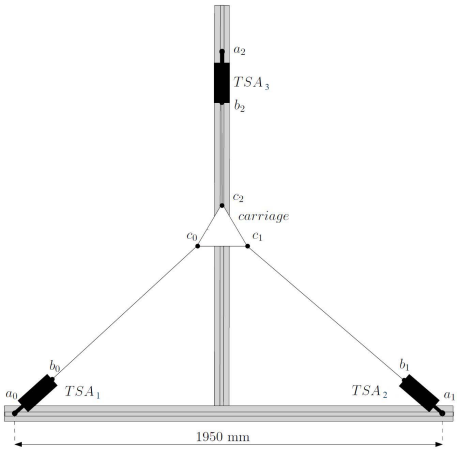

Fig. 3. The 2-D haptic interface setup.

to track the position of the HIC and map it in the end-effector workspace of the remote robot and compute the correct tensile forces for the string of the TSA modules.

1) Preliminary concepts: The HIC position is estimated by means of the encoders in the TSA modules. In fact, the change in length of the twisted strings can be expressed by the number of the motor's shaft revolutions measured by the encoder. Thereafter, the planar position of the HIC can be easily determined considering the lengths of each TSA module's string followed by few trigometric manipulations.

Then, it is worth to highlight that the planar space in which the HIC can move is virtually divided in two circular concentric regions, as illustrated in Fig. 4. In this relation, the position of the end-effector of the remote robot can be controlled using either a position-position mapping or a position-velocity mapping, depending on the region in which the HIC is located. In the inner circular region, a position-position mapping is implemented in order to achieve a precise positioning of the robot end-effector; differently, in the outer circular region, the control switches to a position-velocity mapping in order to produce large translations in the remote robot workspace, while, at the same time, keeping the HIC motions limited to a smaller range of displacements.

2) Position-Position and Position-Velocity Mappings: Let $\mathbf{p}_c$ be the position vector of the center of the HIC in the haptic interface reference frame $\mathcal{F}_{hi}$ and $\mathbf{p}_{eef}$ the position of the end-effector of the remote robot in the robot reference frame $\mathcal{F}_r$ (refer also to Fig. 4). Defining R_1 the radius of the inner circular region and R_2 the radius of the outer circle radius, then the inner and the outer regions can be formally defined by $||\mathbf{p}_c|| < R_1$ and $R_1 < ||\mathbf{p}_c|| < R_2$, respectively. When the HIC is within the inner circular region, the end-effector position of the remote robot $\mathbf{p}_{eef}$ is controlled by "position-position" mapping according to

$$\mathbf{p}_{eef} = \alpha \mathbf{p}_c,$$

where $\alpha \in \mathbb{R}_+$ is a scale factor. Differently, when the HIC is within the outer circular region, a "position-velocity" mapping is implemented, that is the end-effector position is

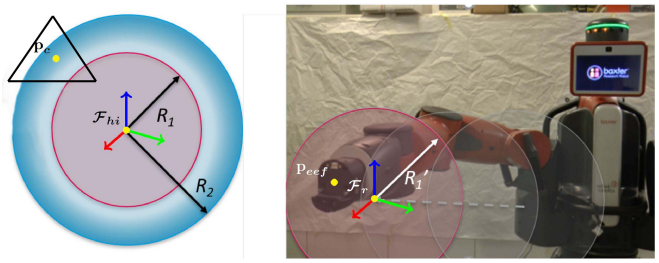

Fig. 4. The position of the HIC in the haptic interface (depicted left) and the position of the end-effector of the remote controlled robot during tele-operation (depicted right)

updated according to

$$\mathbf{p}_{eef} \leftarrow \mathbf{p}_{eef} + T_s \mathbf{v}^*_{eef},$$

where T_s is the sampling time and $\mathbf{v}^*_{eef}$ is the target velocity given by

$$\mathbf{v}^*_{eef} = \frac{\mathbf{p}_c}{||\mathbf{p}_c||} \frac{v_{max}}{R2 - R1},$$

which is proportional to the maximum velocity $v_{max} \in \mathbb{R}_+$.

3) Desired Force Acting on the HIC: The desired force $\mathbf{f}^*$ that the TSA modules have to apply on the HIC is given by the combination of two forces, that is $\mathbf{f}^* = \mathbf{f}^*_1 + \mathbf{f}^*_2$. The first contribution, $\mathbf{f}^*_1$, represents the force exchanged between the teleoperated robot's end-effector and the environment (we assume this force as correctly measured by robot's embedded sensors and available to the controller). The second contribution, $\mathbf{f}^*_2$, is related to the position-velocity mapping case, and is given by

$$\mathbf{f}^*_2 = \begin{cases} -K_2 \frac{\mathbf{p}_c}{||\mathbf{p}_c||} \frac{||\mathbf{p}_c|| - R_1}{R_2 - R_1} & \text{if } R_1 < ||\mathbf{p}_c|| < R_2, \\ -K_2 \frac{\mathbf{p}_c}{||\mathbf{p}_c||} & \text{if } ||\mathbf{p}_c|| \geq R_2, \\ 0 & \text{otherwise,} \end{cases}$$

where $K_2 \in \mathbb{R}_+$ is the stiffness gain, $\frac{\mathbf{p}_c}{||\mathbf{p}_c||}$ is the unit vector that indicate the direction in which the force should be applied on the HIC .

4) Desired Twisted String Tension: Let $\mathbf{l} = \begin{bmatrix} l_0 & l_1 & l_2 \end{bmatrix}$ be the haptic interface joint position vector, where $l_i = ||\mathbf{p}_{c_i} - \mathbf{p}_{a_i}||$ is length of the i-th string plus the TSA module body, expressed as the distance between the string-HIC anchor points $\mathbf{p}_{c_i}$ and the motor-frame attachment points $\mathbf{p}_{a_i}$. Hence, we can write for each string the unit vector $\hat{\mathbf{v}}_i = \frac{\mathbf{v}_i}{||\mathbf{v}_i||} = \frac{(\mathbf{p}_{c_i} - \mathbf{p}_{a_i})}{l_i}$. The force $\mathbf{f}$ acting on the HIC can be expressed as a function of $\hat{\mathbf{v}}_i$ and string tensions:

$$\mathbf{f} = \tau_0 \hat{\mathbf{v}}_0 + \tau_1 \hat{\mathbf{v}}_1 + \tau_2 \hat{\mathbf{v}}_2 = \tau \cdot (J^T)^\dagger,$$

where $(J^T)^\dagger = \begin{bmatrix} \hat{\mathbf{v}}_0 & \hat{\mathbf{v}}_1 & \hat{\mathbf{v}}_2 \end{bmatrix}$ with J the Jacobian matrix, and $\tau = \begin{bmatrix} \tau_0 & \tau_1 & \tau_2 \end{bmatrix}$ the vector of the string tensions of the three TSA modules.

The tension on the strings can now be calculated using the Jacobian matrix J. Once the desired force vector $\mathbf{f}^*$ on the HIC is given, then the force to be exerted by the TSA modules is

$$\tau = J^T \mathbf{f}^* + \lambda \tau^\gamma \quad (1)$$

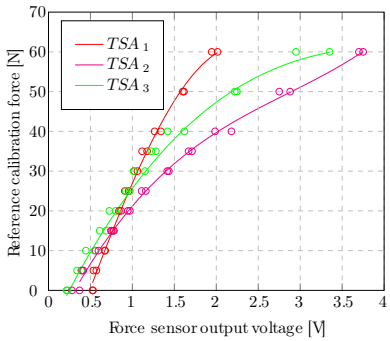

Fig. 5. Calibration curves for the force sensor of the TSA modules.

where the term $\lambda\tau^{\gamma}$ is present in order to always have the strings under tension. Indeed, the vector τ^{γ} is a base of the null space of $(J^T)^{\dagger}$ and λ is defined by

$$\lambda = \max_{i\in\{0,1,2\}} \frac{\tau_i^{min} - \tau_i^*}{\tau_i^{\gamma}} \quad \in \mathbb{R} \tag{2}$$

where τ^{min} is a threshold, τ_i^{γ} is the i-th component of τ^{γ} and τ_i^* is the i-th component of the vector $\tau^* := J^T\mathbf{f}^*$.

III. Experimental Testing and Results

A. TSA Modules Calibration

The first step in order to set up the haptic interface for the experimental evaluation was the calibration of the force sensor embedded in the TSA modules. In detail, for each TSA module the calibration was realized using a linear motor equipped with a commercial load cell in order to provide different reference pulling forces while, at the same time, recording the data of the related output voltage of the force sensor. As shown in Fig. 5, a third-order polynomial curve was numerically computed in order to interpolate the "calibration dataset" to fit the force sensor output voltages with the reference calibration forces in a least-square sense, for the three TSA modules. Note that during this procedure the TSA motor was not powered and the strings kept in the untwisted configuration. Subsequently, the computed force-voltage relations were used online to obtain force measurements to allow the TSA modules apply desired forces thanks to their integrated low-level controller (see also Subsec. II-A).

B. Virtual Wall Environment Test

After the calibration phase described in the previous subsection, the first experimental evaluation performed was the implementation of the haptic perception of a virtual environment consisting in a virtual circular "wall". In particular, since we were considering a bi-dimensional workspace for the haptic interface, this virtual wall was represented by a circle of radius R_2 (see Fig. 6), in which proximity the user of the haptic device should feel a force that impedes her to move outside of the circle – i.e., the circular virtual wall. Note that, in this specific test, the controller for the position-position/position-velocity mappings for the teleoperation of a remote robot described in Sec. II-C was not active – it was used in the teleoperation test described in the next subsection. Here the haptic interface just used the Jacobian matrix to provides a force that pushed back the human operator when she attempted to surpass the circle with radius R_2. This force was proportional to the "deformation" of the virtual wall, the latter characterized by a stiffness K_{wall}.

The behaviour of the system during this test is reported in the graphs of Fig. 6. In relation to this figure, at the beginning the user was required to move the HIC in the positive x direction (refer to Fig. 6, right plot) until she felt the inability to move further due to the presence of the virtual wall, around the instant $t = 8s$ (in the form of a proper resultant force applied on the HIC by the TSA modules). Indeed, in the left-top graph of Fig. 6, it is possible to observe the presence of a force module peak applied by the TSA modules, opposing to the "virtual deformation" of the virtual wall, whereas in the left-bottom graph the revolutions of the output shaft of the three TSA modules are plotted. Then, in the subsequent time instants, this behaviour was repeated 6 times along both the x and y axes alternating positive/negative directions (see the right graph of Fig. 6). After the last touching of the virtual wall along the y axis direction, the user were asked to closely follow the circular wall profile, based on the feeling of the opposing force, for two times in clock and counterclockwise manner: this is observable in Fig. 6 starting from the time instant $t = 60s$, where it is possible to see that the force applied to the HIC oscillated around $20N$, due to the continuous touching of the virtual wall limitation by the user. Still referring to Fig. 6, the imprecise tracking of the force reference value F_{DES} was mainly due to limitations in the dynamics of the TSA modules and the presence of friction. However, in this preliminary test, we consider the functioning of the system sufficiently satisfactory, allowing the user to properly feel the virtual environment via haptic force feedback.

C. Teleoperation Test with Force Feedback

A second experimental evaluation regarded the use of the haptic interface for a teleoperation task. To this purpose, the Baxter robot [29] was used as the remote teleoperated robot of the experiment, in which a user used the haptic device to control the end-point of the Baxter's right arm, according to the position-position and position-velocity mappings, as described in Subsec. II-C (no virtual walls were implemented in this teleoperation test). Additionally, two embedded functionalities already provided by Baxter were exploited: *(i)* the impedance controller which regulates the end-effector pose according to a spatial virtual spring paradigm, in order to have compliance for the interaction with the environment, and *(ii)* the measure of the external force applied to the end-effector when interacting with the environment, in order to provide a force feedback to the user of the haptic device. In Fig. 7 the behaviour of the haptic system during the experiment is reported. In particular, the user was firstly asked to move the Baxter's arm end-point along positive x axis direction. During this motion, the experimenter stopped the robot motion by applying a

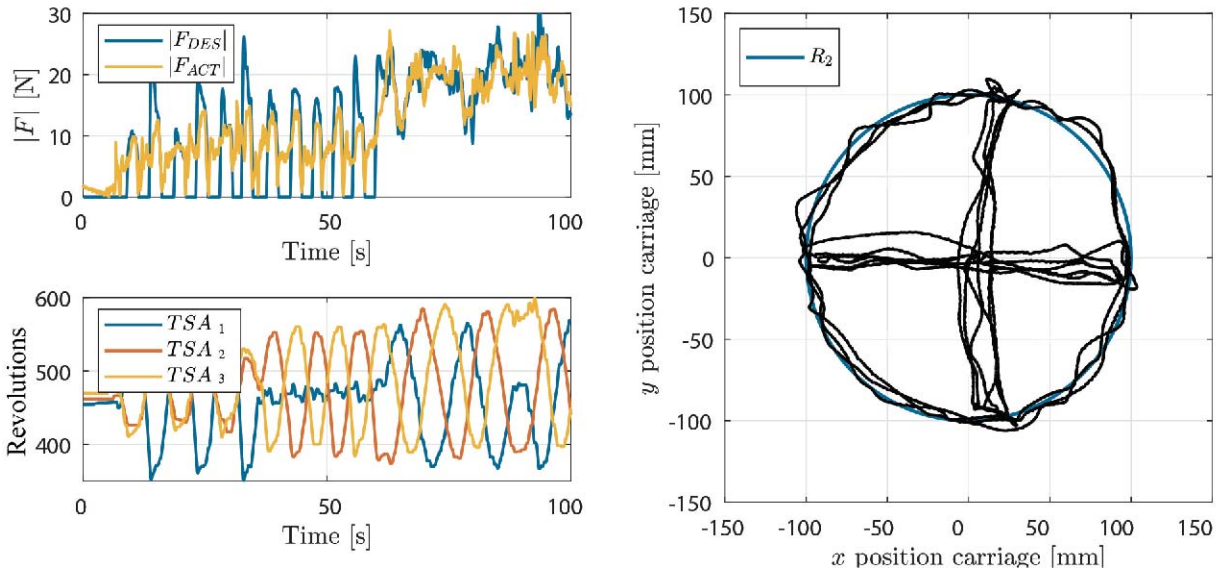

Fig. 6. Behaviour of the haptic interface during the virtual environment test. At first the virtual wall is cyclically probed along the main x and y axis. Then the wall profile is followed circularly several times. Force peaks arise during contacts with the wall.

force (using her arm/hand as an obstacle) to the Baxter's arm end-point: this is clearly visible in the left top graph of Fig. 7 around the instant $t = 30s$, where the force applied on the HIC increased due to external force applied by the experimenter to the teleoperated robot. Note also how, in the left bottom graph around the same time, the rotations of the TSA module's motors are mostly constant, since the user of the haptic device experienced a force that prevented her to continue displacing the HIC. Thereafter, the experimenter quit applying the external force to the robot. Then, the same procedure was repeated along the negative x axis direction: here – as observable by the force increasing around the instant $t = 48s$ – the experimenter again applied an external force, which was therefore felt by the user of the haptic device (it happened for a shorter time.) Finally, still the referring to Fig. 7, two frames of a video recording of the teleoperation test are shown in relation to the application of the external force applied to the robot by the experimenter.

IV. Conclusions

In this paper, a bi-dimensional haptic interface based on the twisted string actuation paradigm has been presented. The study has to be intended as an intermediate step toward the implementation of the 3-D complete haptic interface – theorically designed and simulated in our previous work. The presented system, composed of three TSA modules in order to apply haptic/feedback forces to a human operator, has been illustrated in terms of hardware components, kinematics of the mechanism and control solution for teleoperation purposes. Two simple experiments were performed to test the behaviour of the device preliminarly: the force rendering of a circular virtual wall and the teleoperation of a Baxter robot while feeling the physical feedback of the interaction forces of the robot with the environment. The reported experimental results show that the system is suitable for teleoperation applications with haptic/feedback forces. The outcomes are therefore positive in view of the forthcoming realization of the complete 3-D interface in a future work. Additional future works will also include the improvement of the TSA module performances, in terms of dynamic response and attenuation of friction phenomena for a more effective functioning of the entire teleoperation system.

References

[1] T. B. Sheridan, D. S. Kruser, and S. Deutsch, "Human factors in automated and robotic space systems: Proceedings of a symposium. part 1," 1987.

[2] C. Melchiorri, "Robotic telemanipulation systems: An overview on control aspects," *IFAC Proceedings Volumes*, vol. 36, no. 17, pp. 21–30, 2003.

[3] T. H. Massie, J. K. Salisbury, *et al.*, "The phantom haptic interface: A device for probing virtual objects," in *Proceedings of the ASME winter annual meeting, symposium on haptic interfaces for virtual environment and teleoperator systems*, vol. 55, no. 1. Chicago, IL, 1994, pp. 295–300.

[4] "Geomagic touch," https://www.3dsystems.com/haptics-devices/touch, July 2021.

[5] "Falcon haptic," https://hapticshouse.com/, July 2021.

[6] "Force dimension," https://www.forcedimension.com/, July 2021.

[7] R. Q. Van der Linde, P. Lammertse, E. Frederiksen, and B. Ruiter, "The hapticmaster, a new high-performance haptic interface," in *Proc. Eurohaptics*. Edinburgh University, 2002, pp. 1–5.

[8] Y. Tsumaki, H. Naruse, D. N. Nenchev, and M. Uchiyama, "Design of a compact 6-dof haptic interface," in *Proceedings. 1998 IEEE International Conference on Robotics and Automation (Cat. No. 98CH36146)*, vol. 3. IEEE, 1998, pp. 2580–2585.

[9] S.-U. Lee, H.-C. Shin, and S.-H. Kim, "Design of a new haptic device using a parallel mechanism with a gimbal mechanism," pp. 2331–2336, 2005.

[10] T. Qiu, W. R. Hamel, and D. Lee, "Design and control of a low cost 6 dof master controller," in *2014 IEEE International Conference on Robotics and Automation (ICRA)*. IEEE, 2014, pp. 5313–5318.

[11] S. S. Lee and J. M. Lee, "Design of a general purpose 6-dof haptic interface," *Mechatronics*, vol. 13, no. 7, pp. 697–722, 2003.

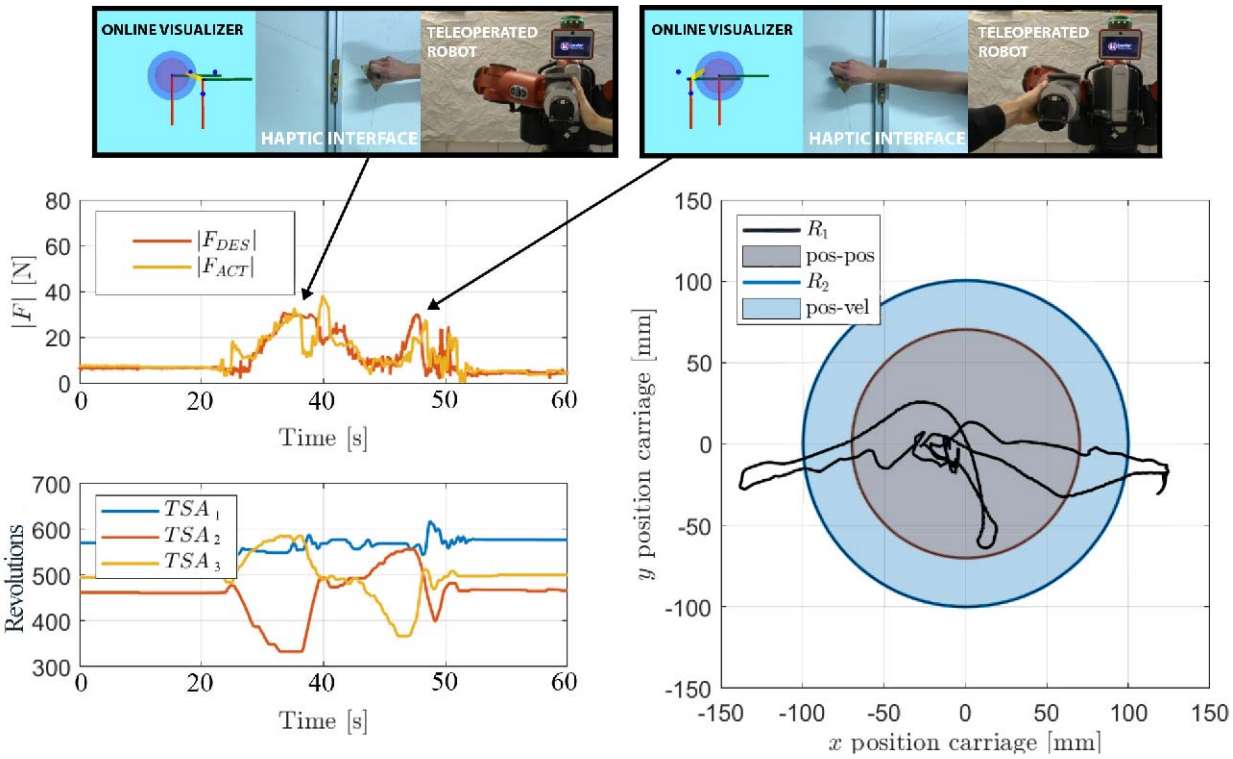

Fig. 7. Behaviour of the haptic interface during the teleoperation test. The feedback force increases the more the handle is brought outside the control sphere R_2. A sudden peak is experienced during contact with an external object or person.

[12] D. Ryu, J.-B. Song, C. Cho, S. Kang, and M. Kim, "Development of a six dof haptic master for teleoperation of a mobile manipulator," *Mechatronics*, vol. 20, no. 2, pp. 181–191, 2010.

[13] K. Oh, W. Z. Rymer, I. Plenzio, F. A. Mussa-Ivaldi, S. Park, and J. Choi, "Development of a planar haptic robot with minimized impedance," *IEEE Transactions on Biomedical Engineering*, vol. 68, no. 5, pp. 1441–1449, 2020.

[14] P. Gallina, G. Rosati, and A. Rossi, "3-dof wire driven planar haptic interface," *Journal of intelligent and robotic systems*, vol. 32, no. 1, pp. 23–36, 2001.

[15] A. Pott, H. Mütherich, W. Kraus, V. Schmidt, P. Miermeister, and A. Verl, "Ipanema: a family of cable-driven parallel robots for industrial applications," in *Cable-Driven Parallel Robots*. Springer, 2013, pp. 119–134.

[16] C. Gosselin, "Cable-driven parallel mechanisms: state of the art and perspectives," *Mechanical Engineering Reviews*, vol. 1, no. 1, pp. DSM0004–DSM0004, 2014.

[17] J. Saint-Aubert, S. Regnier, and S. Haliyo, "Cable driven haptic interface for co-localized desktop vr," in *2018 IEEE Haptics Symposium (HAPTICS)*. IEEE, 2018, pp. 351–356.

[18] J.-H. Park, M.-C. Kim, R. Böhi, S. A. Gommel, E.-S. Kim, E. Choi, J.-O. Park, and C.-S. Kim, "A portable intuitive haptic device on a desk for user-friendly teleoperation of a cable-driven parallel robot," *Applied Sciences*, vol. 11, no. 9, p. 3823, 2021.

[19] Y. Cho, T. Hong, J. Cheong, B.-J. Yi, W. Kim, and H. Jeong, "Development of a new 3t1r type cable-driven haptic device," *Journal of Mechanical Science and Technology*, vol. 34, no. 11, pp. 4721–4734, 2020.

[20] G. Palli, C. Natale, C. May, C. Melchiorri, and T. Wurtz, "Modeling and control of the twisted string actuation system," *IEEE/ASME Transactions on Mechatronics*, vol. 18, no. 2, pp. 664–673, 2012.

[21] T. Sonoda and I. Godler, "Multi-fingered robotic hand employing strings transmission named "twist drive"," in *2010 IEEE/RSJ International Conference on Intelligent Robots and Systems*. IEEE, 2010, pp. 2733–2738.

[22] G. Palli, C. Melchiorri, G. Vassura, U. Scarcia, L. Moriello, G. Berselli, A. Cavallo, G. De Maria, C. Natale, S. Pirozzi, *et al.*, "The dexmart hand: Mechatronic design and experimental evaluation of synergy-based control for human-like grasping," *The International Journal of Robotics Research*, vol. 33, no. 5, pp. 799–824, 2014.

[23] R. Meattini, G. Palli, and C. Melchiorri, "Experimental evaluation of a semg-based control for elbow wearable assistive devices during load lifting tasks," in *2017 International Conference on Rehabilitation Robotics (ICORR)*. IEEE, 2017, pp. 140–145.

[24] R. Shisheie, L. Jiang, L. E. Banta, and M. Cheng, "Design and fabrication of an assistive device for arm rehabilitation using twisted string system," in *2013 IEEE International Conference on Automation Science and Engineering (CASE)*. IEEE, 2013, pp. 255–260.

[25] M. Hosseini, R. Meattini, A. San-Millan, G. Palli, C. Melchiorri, and J. Paik, "A semg-driven soft exosuit based on twisted string actuators for elbow assistive applications," *IEEE Robotics and Automation Letters*, vol. 5, no. 3, pp. 4094–4101, 2020.

[26] I.-W. Park and V. SunSpiral, "Impedance controlled twisted string actuators for tensegrity robots," in *2014 14th International Conference on Control, Automation and Systems (ICCAS 2014)*. IEEE, 2014, pp. 1331–1338.

[27] U. Scarcia, L. Moriello, A. Pepe, G. Palli, and C. Melchiorri, "Design of a twisted-string actuator for haptic force rendering," *IFAC-PapersOnLine*, vol. 51, no. 22, pp. 479–485, 2018.

[28] A. Pepe, M. Hosseini, U. Scarcia, G. Palli, and C. Melchiorri, "Development of an haptic interface based on twisted string actuators," in *2017 IEEE International Conference on Advanced Intelligent Mechatronics (AIM)*. IEEE, 2017, pp. 28–33.

[29] C. Fitzgerald, "Developing baxter," in *2013 IEEE Conference on Technologies for Practical Robot Applications (TePRA)*. IEEE, 2013, pp. 1–6.

[30] H. Dubey and D. Bhope, "Stress and deflection analysis of belleville spring," *IOSR Journal of Mechanical and Civil Engineering*, vol. 2, no. 5, pp. 01–06, 2012.